A Parametric Study of Sheet Metal Denting Using a Simplified Design Approach

Dong-Won Jung*

Department of Mechanical Engineering, Cheju National University, Jeju-do 690-756, Korea

In the interest of improved automotive fuel economy, one solution is reducing vehicle weight. Achieving significant weight reductions will normally require reducing the panel thickness or using alternative materials such as aluminum alloy sheet. These changes will affect the dent resistance of the panel. In this study, the correlation between panel size, curvature, thickness, material properties and dent resistance is investigated. A parametric approach is adopted, utilizing a "design software" tool incorporating empirical equations to predict denting and panel stiffness for simplified panels. The most effective time to optimize an automotive body panel is early in its development. The developed design program can be used to minimize panel thickness or compare different materials, while maintaining adequate panel performance.

Key Words : Denting, Stiffness, Oil Canning, Design, Panel, Parametric Approach

1. Introduction

Predictions of stiffness, denting energy, and critical buckling loads are integral parts of body panel structural design. Body panel performance is described by several different parameters. Stiffness, denting energy and critical buckling load are design criteria for outer body skins. As more stringent CAFE (Corporate Average Fuel Economy) standards are mandated by law, and the emphasis on reduced vehicle weight increases, the design, material, thickness, and processing of every outer body panel needs to be optimized.

High stiffness and good dent resistance are desirable performance features of automotive body panels. These have been largely achieved in the past by evolutionary design, but with the push for lighter weight designs and the introduction of new materials such as aluminum, there is a need for better understanding on an absolute basis. This has been a topic of numerous investigations but because of the complexity of the problem, full understanding is still being pursued. To help advance this, the present study has been undertaken on a parametric basis using highly simplified panels and design analysis to examine the factors that are thought to influence stiffness, denting energy and critical buckling loads.

There has been considerable experimental work on panel stiffness and dent resistance of steels (Johnson Jr. and Schaffnit 1973 ; DiCello and George 1974 ; Burley et al., 1976 ; Rolf et al., 1976); however, there is a lack of data for autobody panels. Vadhavkar et al. (1981) and Mahmood (Swenson Jr. et al., 1982) started using analytical equations to predict dent phenomena. In the following years, much of the efforts for better prediction of panel stiffness and dent resistance have been concentrated on finite element analysis and experimental approach (Sakai et al., 1983 ; Chen and Salamie, 1984 ; Steel, 1991 ; Alaniz, and Borchelt, 1991 ; Shi et al., 1991a ; 1991b ; Krupitzer and Harris, 1992 ; Chen et al., 1993 ; Werner, 1993 ; Shi and Wilczynski 1993 ; Montgomery and Brooks, 1994 ; Van Veldhuizen et al., 1995 ; Vreede et al., 1995 ; Sabbagh et al., 1995 ; Shi et al., 1997). Recent studies have highlighted both the static and dynamic denting characteristics of

* **E-mail** : jdwcheju@cheju.ac.kr
TEL : +82-64-754-3625; **FAX** : +82-64-756-3886
Department of Mechanical Engineering, Cheju National University, Jeju-do 690-756, Korea. (Manuscript **Received** May 11, 2002; **Revised** September 6, 2002)

steels, as in Shi et al.(1977). Experimental examination of both static and dynamic denting of aluminum sheet has been presented by Thorburn (1994). Finite element modelling of dent responses can be found for various static test cases, including work by Chavali & Song (1996) that incorporated a limited re-maping of forming data. Limited work on modelling of dynamic denting can be found in the literature (Vreede et al., 1995; Thomas et al., 1999). Ekstrand & Asnafi (1998) have looked to quantify the effects of structural support boundary conditions on dent resistance to some extent.

Although stiffness is a significant performance feature in its own right, relating to such things as "feel" and flutter and usually specified in terms of a limiting deformation under a given load, it is considered here in combination with denting primarily because it is known that stiffness has a major influence on denting performance. For this purpose, it is more meaningful to define stiffness as the slope of the load-deformation curve at a given load or alternatively as the slope of the straight line from the origin to a given point on the load-deformation curve, referred to as the secant stiffness.

Denting is defined as the residual local deformation of a panel due to a static or dynamic load. Static denting involves a slowly applied force at a point or on a small area such as may occur when an object is placed on a hood or pressed into a fender. Dynamic denting occurs under impact loading such as during a hail storm or collision with a shopping cart. The essential difference is that static denting involves a "slowly" imposed force or deformation while dynamic denting involves a given impact energy. There are no commonly defined or accepted denting performance requirements among automobile manufacturers, nor are individual requirements generally known.

For the study of stiffness, denting and oil canning, a parametric array of panels has been analysed using the design analysis method. And the results of design analysis were compared with finite element analysis for validity. The panels are highly simplified relative to real automobile components but allow variations of those parameters that are thought to influence stiffness and denting. Panels of two sizes are considered, all square in plan and with fixed edges, combined with double curvatures ranging from highly curved (R=100 mm) to flat. Three thicknesses of sheet material typical of automotive panels are considered, with the assumption that there has been no thinning during forming. All the panels are assumed to be AA6111 alloy, but with properties ranging from the T4 condition of the as-rolled sheet to the T8X condition with three levels of forming strain and paint-bake aging. The T8XP condition with enhanced paint-bake response but only one level of forming strain is also considered. The analysis of these panels for deflection under static loading (stiffness) and static and dynamic denting was done with the design software and the commercial finite element code.

2. Theoretical Background

There are various methods available to calculate the design criteria. One of these methods is finite element analysis. The practical application of the finite element method to a design stage is still difficult due to large computation time, unknown boundary conditions and time-consuming preparation of tool data, etc. Also, an iterative process to meet a bogey cannot be incorporated within such an analysis; nor can results be quickly obtained at an interactive terminal. Another methods which can be used are the empirical formula and the spherical shell theory. Using data collected from numerous outer body panels, an empirical formula has been derived to predict the denting phenomena of panels. The latter methods can, however, be incorporated into an iterative technique.

2.1 Stiffness

Stiffness is a primary concern in most outer body panels. The stiffer the panel, the less likely it is to sag under its own weight or when pushed upon. Stiffness can also eliminate panel flutter while driving down the road. The theoretical shell stiffness expression can be written in the following form (Vadhavkar et al., 1981; Lohwasser and

Mahmood, 1979).

$$K=\frac{9.279Et^2H_C\pi^2}{\kappa L_l L_t\sqrt{1-\mu^2}} \tag{1}$$

Where H_C: Total crown height
κ : Spherical shell factor
E : Young's modulus
t : Thickness
μ : Poisson's ratio
L_l: Longitudinal length
L_t: Transverse length

An empirical expression for spherical shell factor is:

$$\begin{aligned}\kappa&=8.06-0.088\frac{H_C}{t} \quad \text{for } \frac{H_C}{t}<20\\ &=6.3 \qquad\qquad\quad \text{for } 20\leq\frac{H_C}{t}\end{aligned} \tag{2}$$

The sweep numbers and chord lengths for an unsupported area of a panel are given. The material determines Young's modulus and Poisson's ratio while the crown height can be calculated from:

$$H_C=\frac{L_l^2}{8R_l}+\frac{L_t^2}{8R_t} \tag{3}$$

Where R_l: Longitudinal radius
R_t: Transverse radius

2.2 Denting energy

Another criteria considered on outer body panels is dent resistance. Poor denting performance can cause permanet damage to the automobile during hail storms. Decklids and hoods can get damaged during slamming. Flying rocks and debris can also cause damage to outer body panels. There are some methods available to calculate the dent resistance criteria. The method currently used is a theoretical comparison formula (Vadhavkar et al., 1981 ; Mahmood and Malik, 1978). This formula computes the relative dent resistance of panels. The higher the denting value, the more resistant a panel would be to denting. The denting energy based on an empirical curve fit (Mahmood 1981 ; Vadhavkar et al., 1981) can be expressed as

$$W\propto\frac{\sigma_y^2t^4}{K} \tag{4}$$

Where σ_y : Yield stress
K : Stiffness
t : Thickness

Then,

$$W=C_1\frac{\sigma_y^2t^4}{K} \tag{5}$$

Where C_1: Constant

Using this equation, the dent resistance of one panel can be compared to another regardless of the value of C_1. Above formula defines a dent as 0.001 inch (0.025 mm) permanent deformation in the panel. The stiffness often tends to control over the dent resistance except when the panel size is small.

2.3 Oil canning

Oil canning is another criterion considered on outer body panels. Oil canning load often controls panel designs over both stiffness and dent resistance. At the present time only one usable form of the oil canning analysis is available (Lohwasser, 1979). Of concern are the degree of oil canning, which determines the likelihood of a panel buckling measured by the parameter λ, and the critical buckling load P_{cr} at which the panel would collapse and reverse its curvature. Oil canning is important to maintain body "feel" in, for instance, roof panels. Oil canning is defined as a nonlinear deflection in the elastic range of a material due to panel geometry. The oil canning parameter is

$$\lambda=\frac{1}{2}\left[\frac{L_lL_t}{t}\sqrt{\frac{12(1-\mu^2)}{R_lR_t}}\right]^{\frac{1}{2}} \tag{6}$$

The lower the λ value, the less likely a panel is to buckle. The critical oil canning load (Swenson Jr. and Traficante, 1982 ; Lohwasser and Mahmood, 1979) is given as

$$R_{cr}=\frac{C_2R_{cr}\pi^2Et^4}{L_lL_t(1-\mu^2)} \tag{7}$$

R_{cr} can be evaluated from

$$R_{cr}=45.929-34.183\lambda+6.397\lambda^2 \tag{8}$$

C_2 can be evaluated from

$$C_2=0.645-7.75\times10^{-7}L_tL_t \text{ in millimeter units}$$
$$=0.645-0.0005L_tL_t \text{ in inch units} \quad (9)$$

Since $C_2<0.0$ for $(L_tL_t)>1290\text{in}^2$, the critical buckling load cannot be calculated for areas greater than 1200 square inches. The designer should determine the minimum critical oil canning load required. Since oil canning is controlled by geometry and modulus of elasticity, it appears that there is no advantage in using high strength steels. However, high strength is necessary to maintain the elastic behavior under large deformations so that an elastic recovery is more likely to occur.

3. Analysis and Results

3.1 Model and Material Properties

Figure 1 shows a schematic of the panel geometry considered. The panels are square with plan dimensions of either 200×200 mm or 600×600 mm. These two sizes are intended to cover the range of unsupported sheet metal in typical panel assemblies. In addition to flat panels, spherical curvatures of 100, 150, 200, 400, 700, 1000, and 4000 mm radius were considered. The sharper curvatures are representative of areas of a fender whereas the flatter curvatures are typical of hoods. Figure 2 shows the stress-strain data used for these calculations. Effective stress versus plastic strain curves were generated from uniaxial tensile data for the materials modelled. As expected, an increase in pre-strain results in a substantial rise in yield stress for the T8X conditions. Tensile data for the T8XP condition was available only for 2% pre-strain. Comparison of the T8X and T8XP flow stress curves for a similar pre-strain reveals a marked increase in yield stress for the T8XP material. The under-aged T4 condition was merely used as a baseline "soft" material for comparison purposes. Table 1 summarizes the material conditions and yield strengths modelled in the current study. Note that the yield values listed are not 2% offset values, but are the proportional limits (the limits of elasticity) specified in the input data used to describe the uniaxial yield behaviour.

Table 1 Yield strength data

Alloy/Temper Designation	Pre-Strain (%)	Yield Strength (MPa)
6111-T4	0	127.
6111-T8X	2.	222.
6111-T8X	5.	252.
6111-T8X	10.	295.
6111-T8XP	2.	261.

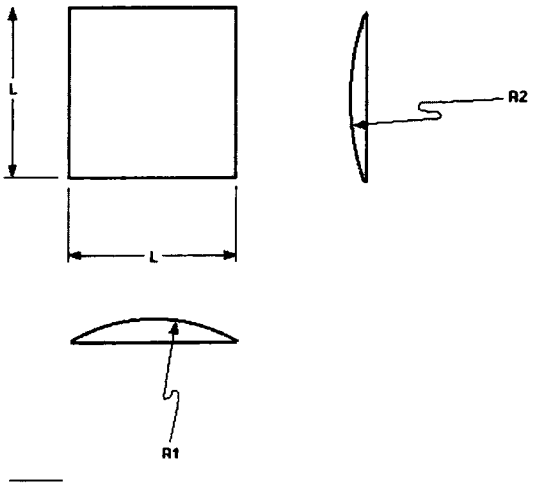

Fig. 1 Schematic of panel geometry adopted in the current study

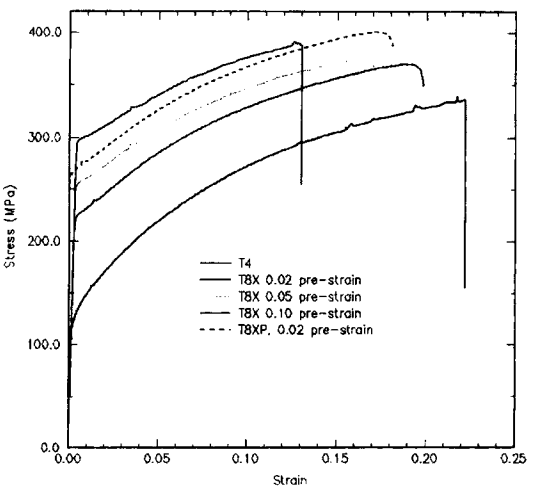

Fig. 2 Stress-strain curves adopted for the sheet materials

It is interesting to note that the effects of heat treatment and pre-strain appear additive and relatively linear for the AA6111 alloy considered. This observation stems from the similar hardening response of the three pre-strain conditions, after allowing for the initial pre-strain. This behaviour suggests that a relatively simple model could be used to describe the hardening kinetics of deformed panels during the paint-bake cycle.

3.2 Finite Element Analysis

In order to validate the design analysis, finite element analysis was also conducted and compared results with the design analysis. Figure 3 and 4 show typical finite element meshes used to model the R4000×R4000, 200 mm panel and the R150×R1000, 600 mm panel, respectively. Quarter-symmetry is utilized to reduce the problem size and extensive mesh focussing is employed near the point of load application or impact as seen in Fig. 5. Four-node Belytschko-Lin-Tsai (Belytschko et al., 1984; Belytschko and Tsay, 1983) elements were used to discretize the panels. Shell elements were chosen over brick elements due to their greater computational efficiency for modelling thin sheets. Unfortunately, the use of shell elements precludes accurate modelling of through-thickness effects due to transverse compression and shear. Neglecting these terms will result in minor errors in predicted dent depth, primarily for low loads or impact velocities. For higher loads, transverse bending and membrane stretching will control the dent response; these terms are accurately modelled using shell elements. Furthermore, the use of brick elements to capture through-thickness terms would also result in a considerably reduced time step and larger mesh sizes requiring prohibitively long computational times.

A 10×10 grid of 1 mm elements is used at the loading point for all of the models. This consistency in local meshing ensures that the interpolation is constant between models and should eliminate any differences between calculations due to discretization errors. Beyond this regular fine-meshed region, transitional meshes are used for the balance of the sheet geometry. Although these transitional meshes varied somewhat between calculations, the strain and stress gradients are low away from the load point and so variations in meshing should not be significant.

Figure 6 shows the mesh used for the impactor in the dynamic denting calculations. The impactor is a 25 mm steel ball bearing. Brick elements were used to discretize the ball and the mesh was focussed somewhat towards the impact face. Note that a rigid body employing only surface discretization near the impact region would likely suffice for these calculations; however, the calculations were not particularly CPU intensive and a fully discretized indentor would better capture the elastic compliance of the sphere.

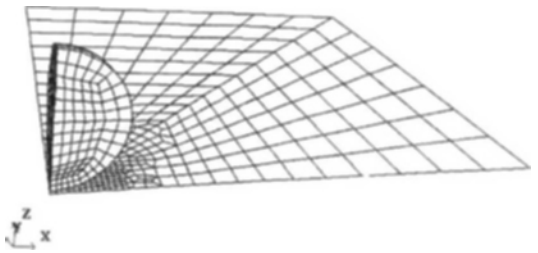

Fig. 3 Finite element mesh used for the R4000×R4000, 200 mm panel

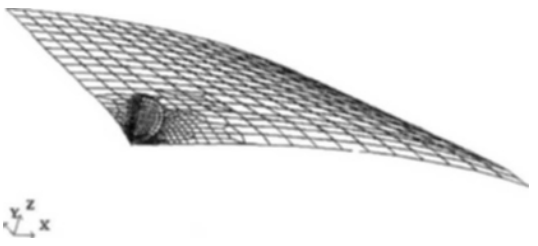

Fig. 4 Finite element mesh used for the R150×R1000, 600 mm panel

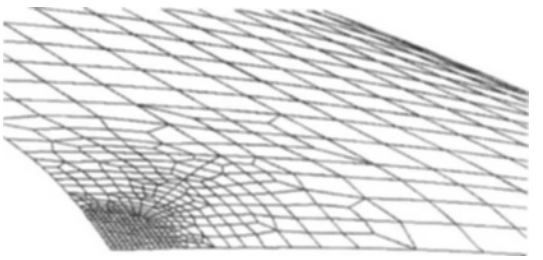

Fig. 5 Close up of mesh in the impact zone showing local refinement

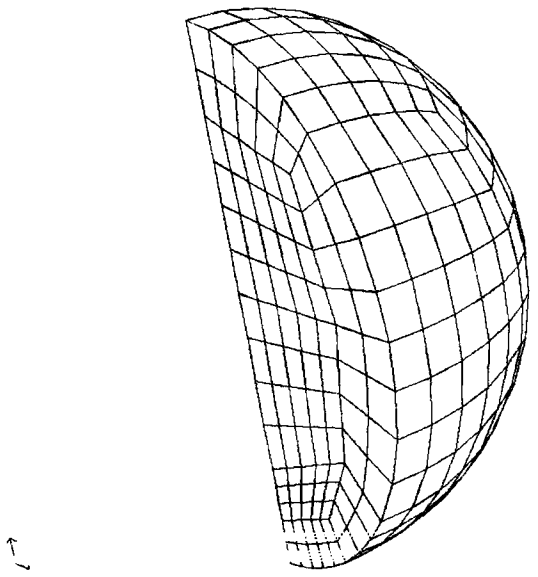

Fig. 6 Finite element mesh used to model impactor

The sheet was modelled as elastic-plastic obeying a Mises yield criterion. Anisotropic yield criteria were not adopted since the plastic strains were small. The steel sphere was modelled as linear elastic with handbook values assigned for the elastic constants. The stress versus plastic strain data was input in a point-wise fashion and linear interpolation was employed between points. Note that LS-NIKE3D currently limits the number of points to eight which is rather small. In this case, the points were concentrated near the initial yield portion of the curve since the strains tended to be relatively low compared, for example, to a forming problem. LS-DYNA3D has no upper limit on the number of points and roughly 50-100 points were used. It is thought that the limited resolution of the stress versus plastic strain curves did not significantly affect the accuracy of the quasi-static LS-NIKE3D calculations since the plastic strains were not large and the problems do not involve flow localization requiring extremely accurate constitutive modelling.

Standard quarter symmetry conditions were imposed along the symmetry planes. The edges of the panels were modelled as fully clamped ; that is, nodal displacements and rotations were suppressed along the outer edges. Adoption of clamped edge conditions will result in a somewhat stiffer response than using simply supported conditions and hence should be conservative in terms of predicted dent depth, at least for the dynamic denting predictions. For the static calculations, a load of 155 N was applied to the center of the panel (38.75 N on the quarter-panel modelled). This load was applied incrementally using 10 steps. The load-point deflections at maximum load and at 10% of maximum (after the first increment) were used to calculate panel stiffness (secant.). Note that a nodal point load was used in the static calculations whereas the performance requirements specify that loading for stiffness measurement is applied through a circular disk and the loading for denting is applied through a sphere. This simplification will result in over-prediction of the actual static deflections and dent depths, but partly counters the effects of the fixed boundary assumption, and was deemed necessary since introduction of the disk-panel and sphere-panel contact conditions would considerably extend and complicate the static analysis.

Table 2 Drop height versus impact velocity (neglecting drag.)

Drop Height (mm)	Impact Velocity (m/s)
204.	2.
1,219.	4.89
2,867.	7.5
5,097.	10.

The dynamic dent calculations considered the impact of a 25 mm steel ball. The impacts were modelled as initial value problems with an initial velocity corresponding to the drop height (Table 2) assigned to the impactor. Penalty function-based contact boundary conditions were defined to enforce intermittent contact between the impactor and panel. The problems were run for a minimum of 5 ms after which the impactor had rebounded off of the panel and the panel was in free vibration. A coupled spring back calculation was then run using LS-NIKE3D to obtain a final deformed shape after "damping" of the vibrational energy.

3.3 Results

The numerical analysis runs were made with the following parametric variations applied to the basic model :

- Panel dimensions of 200×200 and 600×600 mm
- Panel thickness of 0.8, 0.9 and 1.0 mm
- Panel spherical curvatures with radii of 100, 150, 400, 700, 1000, 4000 mm

All results are presented graphically. From the static finite element analysis, panel stiffnesses are shown by plots of load versus displacement, maximum deflection under load, and secant stiffness. Static denting is shown as plots of dent depths versus curvature for one strength and all panel sizes and thicknesses. Dynamic denting is similarly shown by plots of dent depth versus curvature for both sizes and for different strengths. From the design analysis, crown height, static denting energy, secant stiffness and critical buckling load are shown for one strength and all panel sizes, thicknesses and curvatures.

A parametric approach is adopted, utilizing a "design software" tool incorporating empirical equations to predict denting, panel stiffness and critical buckling load for simplified panels. In the conceptual phases of a design, specifically at the inception of the clay model, decisions are rendered and concessions are made which affect the design direction of the entire vehicle. Poor decisions at this early stage will result in inevitable engineering complications downstream. The most effective time to optimize an automotive body panel is early in its development. Consequently, a technique is necessary which will enable rapid analysis of the limited data available during early phase.

In Fig. 7 the predicted crown heights as a function of curvature are plotted for the two sizes of 1 mm AA6111-T8X panels by design analysis. Comparison reveals that the 600 mm panel is much more large crown height than the 200 mm panel. Crown heights increase almost linearly according to the increasing of curvature.

In Fig. 8 the predicted load-deflection curves by finite element analysis are plotted for the two sizes of 1 mm AA6111-T8X panels with a full

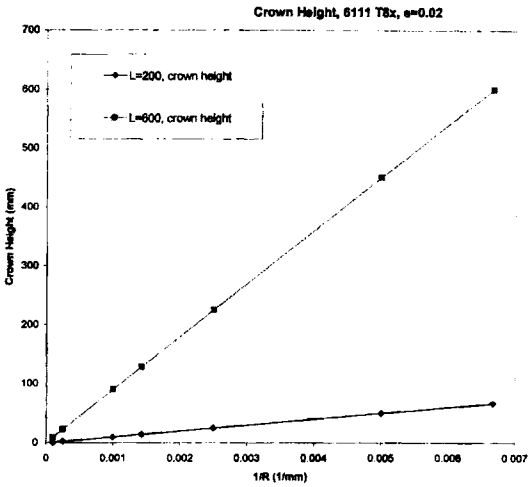

Fig. 7 Crown height as a function of curvature

range of spherical curvatures. The steeper slopes indicate higher geometric stiffening associated with the smaller radii of curvature, as expected. Comparison of Fig. 8(a) and 8(b) reveals that the 600 mm panels are much more compliant than the 200 mm panels. This trend can also be seen in Fig. 9 which plots the maximum load-point deflection for all of the calculations.

The load-deflection responses in Fig. 8(a) and (b) for the large radius of curvature panels (R=4000 mm) display a number of interesting features not seen in the smaller radii panels. The stiffness or slope is initially high, but drops to a minimum at an inflection point and then increases again. This drop in stiffness is associated with oil canning of the panel as the curvature flattens out and inverts. Once the curvature inverts then additional load is carried by tensile membrane stresses with an associated increase in stiffness. The high initial stiffness is due to a compressive membrane action prior to oil canning. The stiffness becomes low during oil canning because the panel supports the applied load primarily in bending with a low flexural rigidity. This low bending stiffness is seen in the flat plate predictions where the load carrying is initially only in bending, with no membrane action until there is significant deflection. The panels with a small radius of curvature resist oil canning beyond the 155 N maximum applied load ; thus they

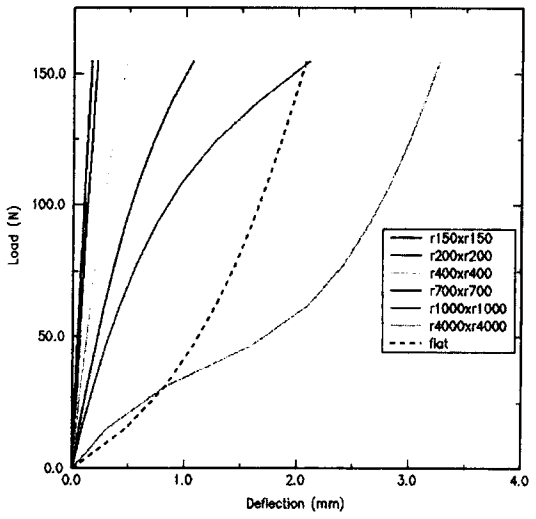

(a) L=200 mm

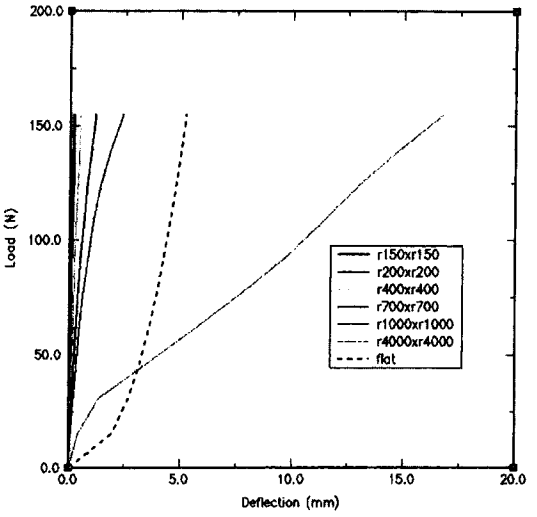

(b) L=600 mm

Fig. 8 Load-displacement response for 6111 T8x, 2% pre-strain, 1 mm panels by finite element analysis

remain stiff since loading is supported through membrane compression. Oil canning and subsequent loss of stiffness can be expected to occur at higher loads.

The effect of panel thickness on maximum deflection or compliance from finite element analysis is also seen in Fig. 9. As expected, the thicker, smaller plates experience lower deflections. The increase in defection for large curvatures is strongly affected by thickness, presumably

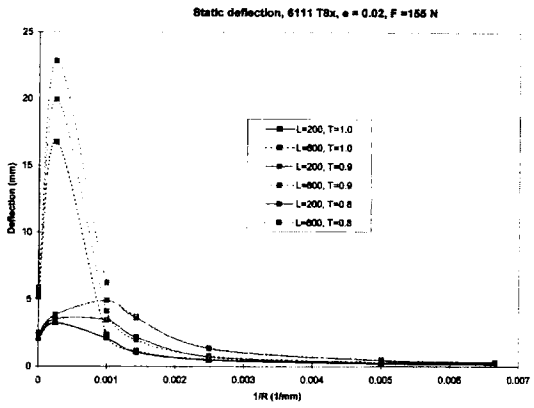

Fig. 9 Maximum load point deflection under a 155 N load by finite element analysis. 6111 T8x, 2% pre-strain

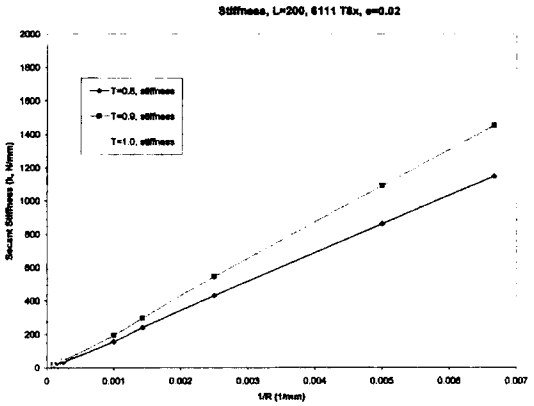

(a) L=200 mm

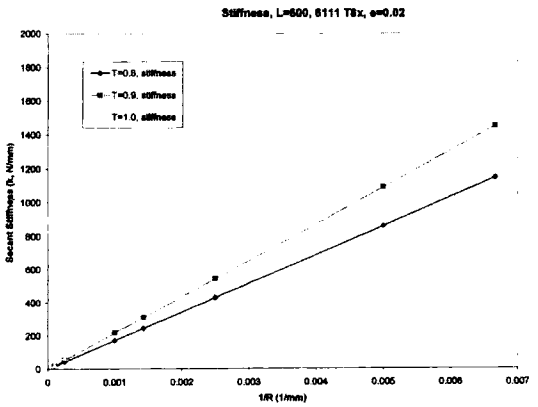

(b) L=600 mm

Fig. 10 Predicted secant stiffness (k) as a function of curvature by design analysis. 6111 T8x, 2% pre-strain

due to the third order dependence of bending

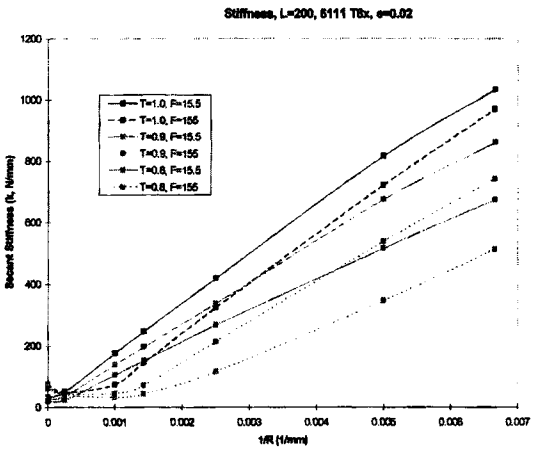

(a) L=200 mm

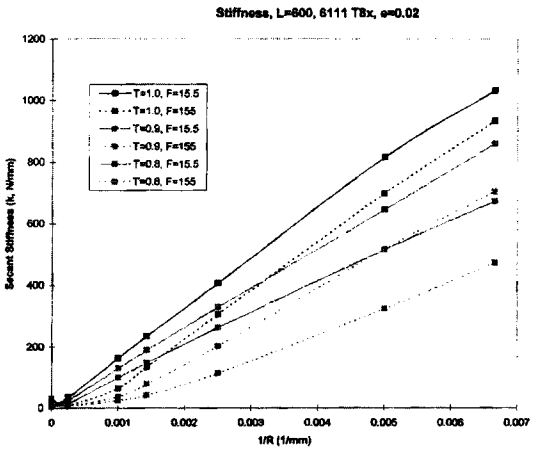

(b) L=600 mm

Fig. 11 Secant stiffness (k) as a function of curvature and thickness by finite element analysis. 6111 T8x, 2% pre-strain

stiffness on thickness.

Predicted panel stiffness values from design analysis are plotted in Fig. 10 as the secant stiffness. Panel stiffness values from finite element analysis are plotted in Fig. 11 as the secant stiffness, calculated as the applied load divided by displacement for loads of 155 N and 15.5 N. For the curved panels, the initial stiffness is higher than the stiffness at maximum load due to the geometric softening as the curvature is reduced by the applied load. The flat plates demonstrate a stiffening response, as described above, due to a transition from bending to membrane tension. But the design analysis could not predict this initial stiffening phenomenon in Fig. 10. Comparison of Fig. 10 and Fig. 11 reveals that the secant stiffnesses calculated by design analysis are more large value than the secant stiffnesses calculated by Finite Element analysis. Figure 11 shows much more rigorous predictions than Fig. 10. But whole trends are consistent well.

Figure 12 plots predicted the denting energy as a function of curvature by design analysis. We can assume that the denting energy stands for the ability of the panel to absorb impact energy. So the higher denting energy panels are able to elastically absorb more impact energy, leaving less energy for the plastic deformation of denting. The energy absorption ability of a panel subject to a given load will correspond to the area under its load-deflection curve. The static load-deflection curves in Fig. 8 indicate that the more sharply curved panels exhibit a stiffer response and absorb less energy for a given load. Consequently, to absorb a given level of impactor kinetic energy, higher contact forces will occur for stiffer panels. When panels have larger radius of curvature, higher denting energy is predicted. In the area of large radius of curvature as shown in Fig. 12, the decreasing rate of denting energy is so quickly. So, we can assume that the changing of curvature for small curvature panels is much more effective. Comparison of Fig. 12(a) and Fig. 12 (b) reveals that the denting energy of 200 mm panels show larger value than 600 mm panels only in case of small curvature because of more large crown height. But larger dynamic dents are predicted for the smaller 200 mm panel compared to the 600 mm panel in case of finite element analysis. This panel size effect is attributed to the lower stiffness and lower dynamic contact forces for the larger panels. Note that panel size has little influence on static dent depth since static load level is not coupled to panel stiffness. So the design analysis can't predict the panel size effect correctly in this case. In case of large curvature, the variation of size and thickness can not affect seriously on denting energy as shown in Fig. 12.

Predicted dent depths by finite element analysis are plotted in Fig. 13 for the AA6111-T8X, 2% pre-strain panels subjected to static loading. Dent

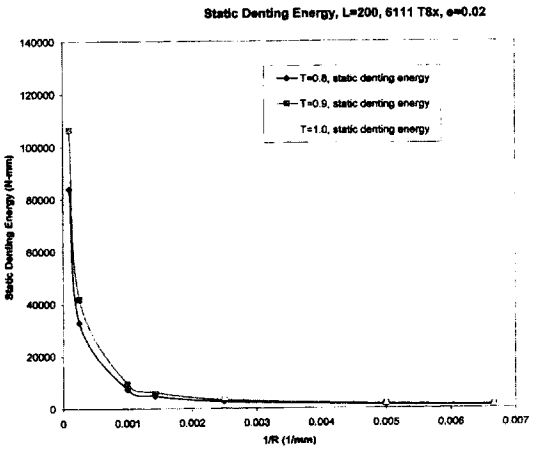

(a) L=200 mm

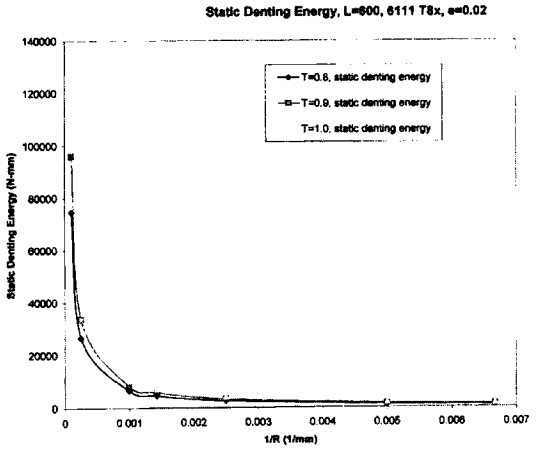

(b) L=600 mm

Fig. 12 Predicted static denting energy as a function of curvature by design analysis. 6111 T8x, 2% pre-strain panels

depth is strongly dependent upon thickness, but not on panel size indicating that it is local bending resistance that controls the depth of static dents for a given material. The sharp curvature panels experience smaller dents since they do not undergo the bending associated with an oil-can mode of deformation. Panels with intermediate curvature exhibited the largest dents since they experience higher bending stresses. In the flatter panels, deflection at lower loads leads to early membrane tension thus minimizing yielding through bending.

Figure 14 plots predicted dent depths after dynamic loading by a 4.89 m/s impact of the 25 mm steel sphere on 1 mm spherical curvature panels with different sizes and strengths. The predictions indicate a marked dependence of dent depth on panel strength. There is also a strong non-linear dependency on radius of curvature with a minimum dent depth occurring for the large radii of curvature. Dent depths are large for the sharply curved panels and also for the flat panels. Interestingly, the local minimum dynamic dent depths occur for radii of curvature corresponding to the maximum static dent depths, as seen by comparing Fig. 13 and 14. These dramatically different behaviours under static and dynamic loading can be attributed to the influence of panel stiffness on the static and dynamic response. Under static conditions, the stiffer panels tend to resist oil canning thereby limiting bending

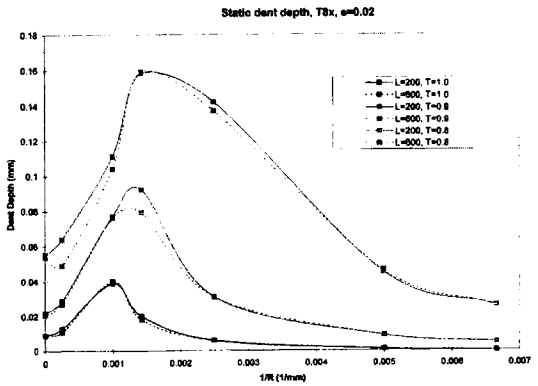

Fig. 13 Static dent depths predicted for the 6111 T8x, 2% pre-strain panels by finite element analysis. Maximum load=155 N

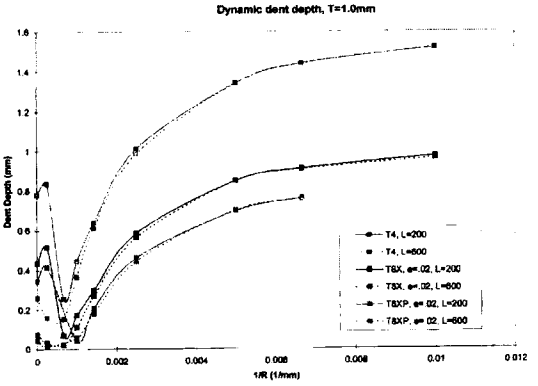

Fig. 14 Dynamic dent depths predicted for the 6111 T8x, 2% pre-strain panels by finite element analysis. Impact velocity=4.89 m/s

stresses and minimizing dent depths. For dynamic loading, the more compliant panels are able to elastically absorb more of the impact energy, leaving less energy for the plastic deformation of denting. The flat panels also show a stiffer response than the R4000×R4000 panels which again leads to higher contact forces and the larger dent depths seen in Fig. 14.

Contact force-time histories for an impact velocity of 4.89 m/s are plotted in Fig. 15 for the 1 mm AA6111-T8X, 2% pre-strain panels. High contact forces approaching 600 N are attained for the more sharply curved panels. The magnitude of the force decreases and the duration increases as the radii of curvature increase. These general trends are consistent with the load-deformation and stiffness trends seen in Fig. 8 and 11, respectively. The flat plates exhibit a lower contact force early in the impact; but later in the impact period, the contact force increases sharply. The lower initial forces are attributed to the low initial stiffness of flat panels seen in Figs. 8 and 11. The stiffness increases sharply later during the impact as reflected by the hardening of the flat panel load-deformation curves in Fig. 8.

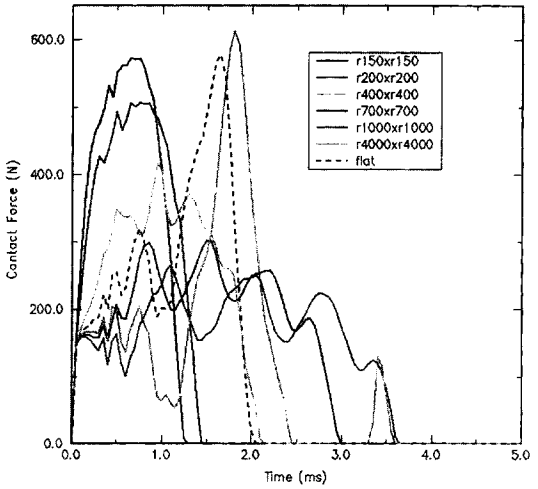

(a) L=200 mm

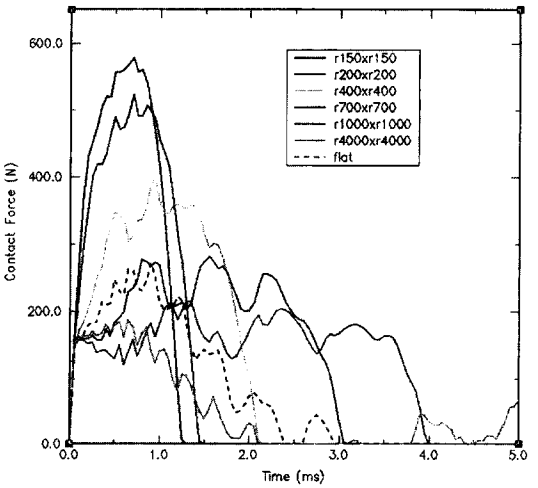

(b) L=600 mm

Fig. 15 Contact force histories for the 1 mm, 6111 T8x, 2% pre-strain panels, Impact velocity= 4.89 m/s

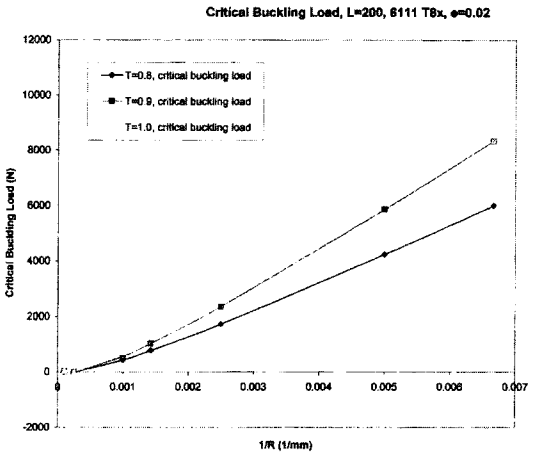

(a) L=200 mm

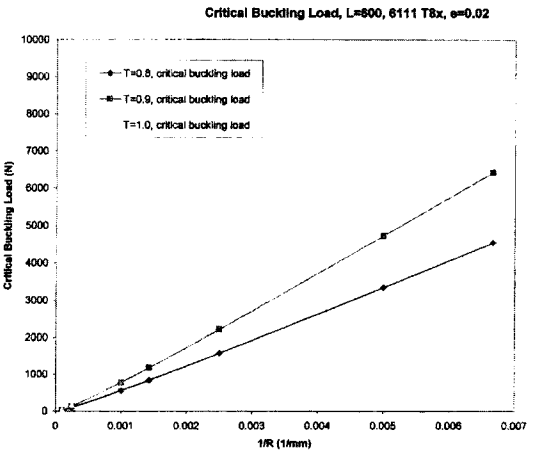

(b) L=600 mm

Fig. 16 Predicted critical buckling load as a function of curvature by design analysis. 6111 T8x, 2% prestrain panels

Figure 16 shows that predicted critical buckling load as a function of curvature by design analysis. Higher curvature, smaller size and thicker panels are more safe from oil canning phenomena as shown in Fig. 16. Design analysis can supply easily and quickly so useful data, e.g. critical buckling loads, static denting enegy and secant stiffness etc., for the conceptual phases of a design.

4. Discussion and Conclusions

In present study, the theory of design analysis was described and the results of design analysis have been compared with those of finite element analysis for validity. The present study has served to demonstrate the complex interdependence of the denting, stiffness and oil canning response of body panels to material strength, thickness, panel size, curvature, support condition, and loading by using the developed design code and the commercial finite element code. Panel stiffness and static dent performance are enhanced by curvatures which favor membrane loading as opposed to bending.

Static and dynamic dent resistance improve with increased panel thickness and material yield strength. Panels of high local curvature and stiffness will perform well under static loading, but will be susceptible to poor dynamic dent performance due to an inability to elastically absorb the kinetic energy of an impacting body. Designers must be aware of this competition in optimization and trade-off studies involved in panel design.

In addition to extending the present analytical design tools, it may also be desirable to create finite element-based analysis tools for the prediction of denting that consider entire panels with their actual supports. Such models would incorporate both inner and outer panel geometry, supporting inter-connections, and attachment points. In addition, effective plastic strains and residual stresses (possibly) could be incorporated from forming simulations considering the outer panel. Strain information, along with knowledge of paint-bake response, would then be used to predict local yield stresses within the outer panel. The availability of such detailed information should greatly improve the fidelity of dent and stiffness predictions and would be of use in design acceptance exercises as well as optimization and down-gauging studies. Conclusions are summarized as following ;

(1) The design analysis can't predict initial stiffening phenomenon and show much less rigorous predictions than the finite element analysis. The secant stiffnesses calculated by design analysis have larger values than those calculated by the finite element analysis. But whole trends are consistent so well.

(2) The design analysis can predict the denting energy. And the denting energy stands for the ability of the panel to absorb impact energy. So the more high denting energy panels are able to elastically absorb more of the impact energy, leaving less energy for the plastic deformation of denting.

(3) The design analysis can't predict the panel size effect correctly in small curvature case. In case of large curvature, the variation of size and thickness can not affect seriously on denting energy.

(4) The design analysis can predict critical buckling load and show that higher curvature, smaller size and thicker panels are more safe from oil canning phenomena.

(5) The design analysis can supply easily and quickly so useful data, e.g. critical buckling loads, static denting enegy and secant stiffness etc., for the conceptual phases of a design.

Acknowledgment

This work was supported by Korea Research Foundation Grant. (KRF-2001-002-E00018)

References

Alaniz, C. L. and Borchelt, J. E., 1991, "Study of Parameters that Affect Body Panel Performance Predictions," SAE Paper No. 910289.

Belytschko, T., Lin, J. I. and Tsay, C., 1984, "Explicit Algorithms for the Non-Linear Dyna-

mics of Shells," *Computer Methods in Applied Mechanics and Engineering*, Vol. 42, pp. 225~251.

Belytschko, T. and Tsay, C., 1983, "A Stabilization Procedure for the Quadrilateral Plate Element with One-Point Quadrature," *International Journal for Numerical Methods in Engineering*, Vol. 19, pp. 405~419.

Burley, C. E. and Niemeier, B. A., 1977, "Denting Properties of Aluminum Autobody Components," SAE Technical Paper No. 770199.

Burley, C. E., Niemeier, B. A. and Koch, G. P., 1976, "Dynamic Denting of Autobody Panels," SAE Technical Paper No. 760165.

Chavali, R. and Song, W., 1996, "Coupling Forming and Denting Simulations for Automotive Closure Panels".

Chen, C. H., Rastogi, P. K. and Horvath, C. D., 1993, "Effects of Steel Thickness and Mechanical Properties on Vehicle Outer Panel Performance: Stiffness, Oil Canning Load and Dent Resistance," *Proceedings IBEC '93, International Body Engineering Conference*, pp. 26~32.

Chen, K. K. and Salamie, P. A., 1984, "A Mathematical Model for Calculating the Dent Initiation Loads at the Door Centers," SAE Paper No. 841201.

DiCello, J. A. and George, R. A., 1974, "Design Criteria for the Dent Resistance of Auto Body Panels," SAE Technical Paper No. 740081.

Ekstrand, G. and Asnafi, N., 1998, "On Testing of the Stiffness and the Dent Resistance of Autobody Panels," *Materials and Design* 19.

Johnson Jr., T. E. and Schaffnit, W. O., 1973, "Dent Resistance of Cold-Rolled Low-Carbon Steel Sheet," SAE Paper No.730528.

Kohmura, S. and Urbanek, J., 1977, "Dent Resistance of Aluminum Alloy Sheets," Alcan International Ltd., KRDC Report, KR-77/044.

Krupitzer, R. P. and Harris, R. P., 1992, "Improvements in the Dent Resistance of Steel Body Panels," SAE Technical Paper No. 920243.

Lohwasser, A. K. and Mahmood, H. F., 1979, "Surface Panel Oil Canning Anlysis-Theoretical Development," *Technical Memorandum*, No. 9-611, Chrysler Corp..

Mahmood, H. F., 1981, "Dent Resistance of Surface Panel and Slam Area," SAE Technical Paper No. 810099.

Mahmood, H. F. and Malik, D., 1978, "Dent Resistance of Surface Panel and Slam Area," *Technical Memorandum*, No. 8023, Chrysler Corp..

Montgomery, J. and Brooks, A., 1994, "Influence of Geometry on Outer Panel Dent Resistance as Demonstrated Through FEA," *Proceedings IBEC '94, International Body Engineering Conference, September 26-29*, Detroit, Michigan, pp. 85~89.

Neimeier, B. A. and Burley, C. E., 1978, "Hailstone Response of Body Panels-Real and Simulated," SAE Paper No. 780398.

Rolf, R. L., Sharp, M. L. and Stroebel, H. H., 1976, "Structural Characteristics of Aluminum Body Sheet," SAE Technical Paper No. 770200.

Sabbagh, M. A., Chavali, R. N. and Montgomery, J. S., 1995, "Quasi-Static Dent Depth Simulation Usin Non-Linear FEA," *Proceedings IBEC '95, International Body Engineering Conference*, pp. 87~90.

Sakai, H., Saito, K. and Tsukada, H., 1983, "Stiffness and Dent Characteristics of Body Outer Surface Panel-Finite Element Analysis and Experiment," *Int. J. of Vehicle Design*, Vol. 4, No. 1, pp. 13~22.

Shi, M. F. and Wilczynski, J. S., 1993, "Potential Weight Savings Versus Dent Resistance Performance of High Strength Steel Body Panels," *Proceedings IBEC '93, International Body Engineering Conference*, pp. 37~43.

Shi, M. F., Brindza, J. A., Michel, P. F., Bucklin, P., Belanger, P. J. and Prencipe Jr., J. M., 1997, "Static and Dynamic Dent Resistance Performance of Automotive Steel Body Panels," SAE Paper No. 970158.

Shi, M. F., Meuleman, D. J., Alaniz, C. L. and Zurdosky, S. J., 1991, "An Evaluation of the Dynamic Dent Resistance of Automotive Steels," SAE Paper No. 910287.

Shi, M. F., Meuleman, D. J., Alaniz, C. L. and Zurdosky, S. J., 1991, "Pre-Strain Effects on Static Dent Resistance of Automotive Steels," SAE Paper No. 910288.

Steel, T. N., 1991, "Bake Hardening Steel Ap-

plication Study-Key Factors of Dent Resistance Impovement" SAE Technical Paper No. 910291.

Swenson Jr., W. E. and Traficante, R. J., 1982, "The Influence of Aluminum Properties on the Design, Manufacturability and Economics of an Automotive Body Panel," SAE Paper No. 820385.

Thomas, D., Hodgins, R. B., Worswick, M. J., Oddy, A. S., Gong, K., Finn, M., 1999, "FEM Technique for Static & Dynamic Dent Modelling of Aluminum," *Proceedings of Numisheet' 99-Volume 1*, Gelin, J. C. and Picart, P., Eds., pp. 367~372.

Thorburn, H. J., 1994, "Comparitive Tests of Stiffness and Dent Resistance on Aluminum and Steel Fenders," *Proceedings IBEC '94, International Body Engineering Conference, September 26-29*, Detroit, Michigan, pp. 105~112.

Vadhavkar, A. V., Fecek, M. G., Shah, V. C. and Swenson, W. E., 1981, "Panel Optimization Program (POP)," SAE Paper No. 810230.

Van Veldhuizen, B., Kranendonk, W. and Ruifrok, R., 1995, "The Relation Between the Curvature of Horizontal Automotive Panels, the Panel Stiffness and the Static Dent Resistance," *Proceedings IBEC '95, International Body Engineering Conference*, pp. 62~70.

Vreede, P. T., Tamis, P. J. and Roelofsen, M. E., 1995, "The Influence of Material Properties and Geometry on Dynamic Dent Resistance : Experiments and Simulations," *Proceedings IBEC '95*, International Body Engineering Conference, pp. 79~86.

Vreede, P. T., Tamis, P. J., Roelofsen, M. E., 1995, "The Influence of Material Properties and Geometry on Dynamic Dent Resistance : Experiments and Simulations," *IBEC*.

Werner, M. F., 1993, "Finite Element Simulation of Steel Body Panel Performance for Quasi-Static Dent Resistance," *Proceedings IBEC '93, International Body Engineering Conference*, pp. 33~36.